

$$\delta_n = 10\%$$

The counter electromotive force of the motor is

$$C_e = \frac{U_N - I_N R_a}{n_N} = \frac{870 - 3100 \times 0.01}{50} \quad (1)$$

$$= 16.78 \text{V} \cdot \text{min}/r$$

The moment coefficient is

$$C_m = \frac{30}{\pi} C_e = 9.55 \times 16.78 = 160 \text{V} \cdot \text{min}/r \quad (2)$$

The armature current time constant of the motor is

$$T_l = \frac{L_a}{R_a} = \frac{1.851}{0.01} = 0.185 \text{s} \quad (3)$$

The electrical and mechanical time constant of electric drive system is

$$T_m = \frac{GD^2 R}{375 C_e C_m} = \frac{4gJR}{375 C_e C_m} \quad (4)$$

$$= \frac{4 \times 9.81 \times 32625 \times 0.01}{375 \times 16.78 \times 160} = 0.0127 \text{s}$$

B Design of The Double Closed-Loop Speed Regulating System

According to engineering design methods, the double closed-loop DC speed regulating system controller can be designed to meet the requirements.

The main drive system of the 1750mm four-high rolling mill adopts two three-phase-bridge rectifier circuits in parallel to form a 12-pulse power feeding equipment. This part of the transfer function of the filter can be indicated by an order inertia link. The filter time constant T_s can be selected as 0.0017s.

Design of current regulator

The control voltage U_i^* is designed in the range of 0-10V, the armature voltage U_{a0} of the DC motor is 0-870V. So the magnification coefficient of the rectifier is $K_s = 870/10 = 87$. Considering the wave front time is 1.67ms, the filter time constant of the current feedback link is set at $T_{oi} = 1 \text{ms} = 0.001 \text{s}$

The feedback coefficient of the current loop is

$$\beta = \frac{U_i^*}{\lambda I_N} = \frac{10}{1.25 \times 3100} = 0.00258 \text{V/A} \quad (5)$$

Judging from the steady state requirements, in order to get the ideal stall characteristics, we hope that the current has no static error. According to the dynamic requirements, in the actual system, the armature current system is not allowed with much overshoot during sudden

action. So as to ensure the current in the dynamic process does not exceed the allowable value. To this end, the current loop should follow nature-based. I type of system should be used [12-13]. Since the current loop control object is a double inertia, to be corrected as typical system, PI type current regulator should be used apparently. The transfer function can be expressed as

$$W_{ACR}(s) = \frac{K_i(\tau_i s + 1)}{\tau_i s} \quad (6)$$

Where K_i is the scale factor of the current regulator; τ_i is ahead of the current time constant of the regulator.

As can be seen from the formula (6), the current regulator parameter K_i and τ_i are still unknown. In order that the zero of regulator can be neutralized by the great time constant of the controller object, choose $\tau_i = T_l = 0.185 \text{s}$, then the only one unknown parameter is the scaling factor K_i

So the typical form of the current loop is converted to

$$K_I = \frac{K_i K_s \beta}{\tau_i R_a} \quad (7)$$

The minimum time constant of the current loop is the sum of $T_{\Sigma i}$, in accordance with the small time constant approximation process, taking

$$T_{\Sigma i} = T_s + T_{oi} = 0.0017 \text{s} + 0.001 \text{s} = 0.0027 \text{s}$$

Depending on the required dynamic performance, the exception of the design of the current overshoot is $\delta_i \leq 5\%$. According to the condition, $\xi = 0.707$,

$$K_I T_{\Sigma i} = 0.5$$

So the open loop gain is designed as

$$K_I = 0.5 / T_{\Sigma i} = 0.5 / 0.0027 = 185 \quad (8)$$

So the scale factor for the ACR is

$$K_i = \frac{K_I \tau_i R_a}{K_s \beta} = \frac{185 \times 0.185 \times 0.01}{87 \times 0.00258} = 1.525 \quad (9)$$

Then, the current loop ACR regulator can be expressed as

$$W_{ACR}(s) = \frac{1.525(0.185s + 1)}{0.185s} \quad (10)$$

C Design of speed regulator

The feedback factor of the speed loop voltage is $\alpha = u_N / n_N = 10 / 50 = 0.2 \text{V} \cdot \text{min}/r$

In order to achieve speed static error, so the speed open loop transfer function should consist two integral parts, so it should be designed to type II system I_d , such a system should meet the requirements of good performance for dynamic Immunity^[14]. Thus, ASR PI regulator should be adopted. The transfer function is

$$W_{ASR}(s) = \frac{K_n(\tau_n s + 1)}{\tau_n s} \quad (11)$$

The transfer function of the open-loop speed control system is

$$W_n(s) = \frac{K_n(\tau_n s + 1)}{s^2(T_{\Sigma n} s + 1)} \quad (12)$$

Where the open loop gain is

$$K_n = \frac{K_n \alpha R_a}{\tau_n \beta C_e T_m} \quad (13)$$

So the closed loop gain is

$$K_n = \frac{(h+1)\beta C_e T_m}{2h\alpha R_a T_{\Sigma n}} \quad (14)$$

After simplified, the current loop can be regarded as a part of the speed loop; the equivalent time constant of the current loop is $1/K_I$. According to the ripple size of the tachometer, the filter time constant of the speed loop can be determined as $T_{on} = 0.01s$. So the small time constant of the speed loop can be determined by

$$T_{\Sigma n} = \frac{1}{K_I} + T_{on} = \frac{1}{185} s + 0.01s = 0.0154s$$

Depending on the principle of both follow resistance and immunity performance are good. $h = 5$. The ahead time constant of ASR can be determined as

$$\tau_n = hT_{\Sigma n} = 5 \times 0.0154s = 0.077s$$

The closed loop gain is designed as

$$\begin{aligned} K_n &= \frac{(h+1)\beta C_e T_m}{2h\alpha R_a T_{\Sigma n}} \\ &= \frac{6 \times 0.00258 \times 16.78 \times 0.0127}{2 \times 5 \times 0.2 \times 0.01 \times 0.0154} = 10.71 \end{aligned} \quad (15)$$

Then the speed loop controller ASR can be expressed as

$$W_{ASR}(s) = \frac{10.71(0.077s + 1)}{0.077s} \quad (16)$$

III. SIMULATION AND RESULTS ANALYSIS

According to the above parameters that calculated by the methods of engineering design. A specific model of the main drive speed control system is designed. The model is tested in MATLAB simulation platform. Simulation results for the drive system are shown in the following figures. Simulation curves shown in Fig. 2 are the current simulation results. The speed simulation results are shown in Fig. 3. The current loop feedback voltage U_i simulation results are shown in Fig. 4. The speed loop feedback voltage U_n simulation results are shown in Fig. 5.

The simulation graphs show that at the moment the motor starts the armature current increases instantly. However, due to mechanical and electrical inertia, the speed of the motor will not grow quickly. Because the value of the input offset voltage ΔU_n for the speed regulator ASR is still large, so the output voltage keep the limiting value forcing the armature current remains a rapid rise. Until $I_d \approx I_{dm}, U_i \approx U_{im}^*$, the growth of I_d is suppressed by the current regulator. At the same time, ASR enters and keeps saturation. However, ACR is not saturated generally.

When the speed rises to the given value $n^* = n_N = 50rpm$. The input bias of the ASR speed regulator reduces to zero. Due to the integral action, the motor is still accelerating, resulting in speed overshoot. After speed overshoot, ASR begins to withdraw from saturation. U_d and I_d start to decrease quickly, the speed keeps on rising as long as I_d is larger than I_{dl} . When the motor starts, the current loop feedback voltage U_i is the biggest value 12V, the speed closed-loop feedback voltage U_d is the least value 0V, along with the speed increases, the current decreases. Until the speed reaches the maximum value, both the armature current and the current loop feedback voltage decrease to minimum value. When the speed reaches a peak, the motor begins to slow down under the load resistance, at the same time, the armature current also decreased rapidly until stable^[15-16]. Finally, both the armature current and the speed reach steady state. The armature current reaches at the rated 3100A, the speed reaches and keeps at the rated 50rpm. Both the current loop feedback voltage and the speed loop voltage reach steady state.

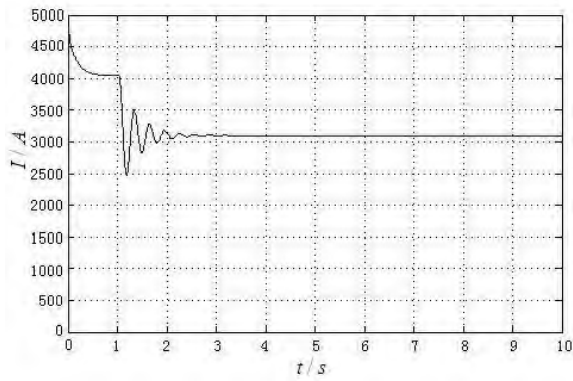


Figure 2. The curve of current simulation

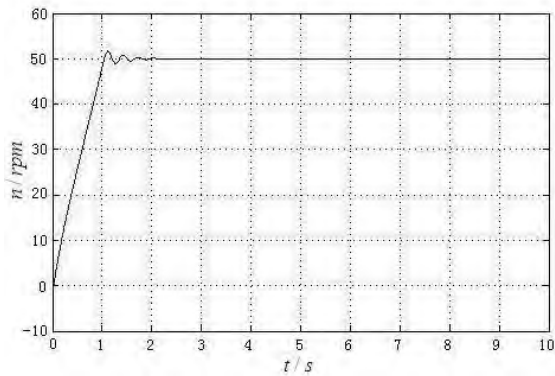


Figure 3. The curve of speed simulation

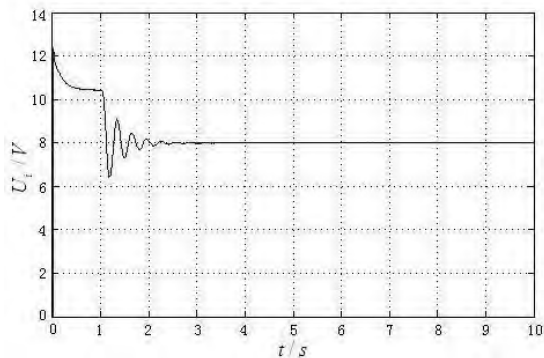


Figure 4. The curve of current loop feedback voltage simulation

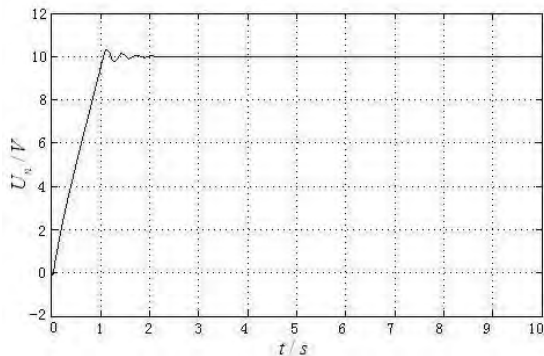


Figure 5. The curve of speed feedback voltage simulation

IV. CONCLUSIONS

The double-loop control system designed in this paper applies to the main drive speed regulating system has a good control effect.

REFERENCES

- [1] C. Bettles and M. Barnett. Sachdev. *Advances in Wrought Magnesium Alloys-Fundamentals of processing, properties and applications* [M]. Cambridge :Woodhead PublishingLtd,2012.
- [2] Mathis K, Trojanova Z, Lukac P, Cáceres CH etc. Modeling of hardening and softening processes in Mg alloys[J]. *Journal of Alloys and Compounds*,2004,378:176-179.
- [3] Dreyer CE, Chiu WV, Wagoner RH and Agnew SR. Formability of a more randomly textured magnesium alloy sheet: Application of an improved warm sheet formability test[J]. *Journal of Materials Processing Technology*. 2010,210: 37-47.
- [4] Staroselsky A and Anand L. A constitutive model for hcp materials deforming by slip and twinning: application to magnesium alloy AZ31B[J]. *International Journal of Plasticity*,2003,19: 1843-1864.
- [5] Wang Y, Chen LQ, Liu ZK and Mathaudhu SN. First-principles calculations of twinboundary and stacking-fault energies in magnesium[J]. *Scripta Materialia*,2010,62: 646-649.
- [6] Sun Yin-kang. *Cold rolled strip mill model and control*[M]. Beijing: Metallurgical Industry Press,2010.1.(Chinese).
- [7] Yong-jiang ZHENG, Author Vitae,Guang-xian SHEN. Spatial Vibration and Its Numerical Analytical Method of Four-high Rolling Mills [J].*Journal of Iron and Steel Research*, Internal ,2004 ,21(9):837-843.
- [8] Mohamed S. Zaky. A self-tuning PI controller for the speed control of electrical motor drives[J]. *Electric Power Systems Research* ,2015,119,unpublished.
- [9] Li Heng, and Han Xiang-feng. Matlab simulation of fuzzy PID Double Loop DC Motor Control System Based[J]. *Coal Mine Modernization*,2009,9(10):66-68.[Chinese]
- [10] P. Krishnamurthy, F. Khorrami .Voltage-fed permanent-magnet stepper motorcontrol via position-only feedback[J].*Control Theory Press*,Aug.2004 ,pp499-510,doi:10.1049/ip-cta:20040622.
- [11] F. Betin, M. Deloizy, C. Goedel. Closed loop control of stepping motor drive: comparison between PID control, self tuning regulation and fuzzy logic control[J].*Eur. Power Electron*,1991,8(1-2):33-39.
- [12] W. Kim, C. Yang, C.C. Chung. Design and implementation of simplefield-oriented control for permanent magnet stepper motors without DQ trans-formation[J]. *IEEE, Magnetics Society, Press*,Oct. 2011, pp4231-4234,doi: 10.1109/TMAG.2011.2157956.
- [13] Chen D and Segorg DE. PI/PID controller design based on direct synthesis and disturbance rejection[J]. *Industrial & Engineering Chemistry Research*, 2002,41(19):4807-22
- [14] Cai YH, Qi RY, Cai J, Deng ZQ. Online modeling for switched reluctance motor using radial basis function neural network and its experimental validation[J]. *Acta Aeronautica et Astronautica Sinica* ,2012,33(4): 705-14.(Chinese)
- [15] Chen Bo-shi. *Electric Drive Automatic Control System - Motion Control System*[M]. Beijing: Machinery Industry Press,2003.(Chinese)
- [16] Zhang Chong-wei. *Motion Control System*[M]. Wuhan: Wuhan University of Technology Press,2002. (Chinese)